PII: S0955-2219(96)00184-7

Cyclic Fatigue-Crack Propagation in SiC-Whisker-Reinforced Y-TZP Composites

Guo-Dong Zhan,[a] Yi-Zeng Zhang,[b] Jian-Ling Shi[a] & Tung-Sheng Yen[a]

[a]Shanghai Institute of Ceramics, Chinese Academy of Sciences, Shanghai 200050, People's Republic of China
[b]Department of Materials Science and Engineering, Huazhong University of Science and Technology, Wuhan 430074, People's Republic of China

Abstract

The ambient-temperature subcritical growth behaviour of SiC-whisker-reinforced yttria-stabilized zirconia (SiCw/3Y-TZP) ceramic composites is investigated during cyclic fatigue loading. Based on long-crack experiments using four-point bending specimens, cyclic fatigue crack growth rates (over the range 10^{-10} to 10^{-5} (m/cycle)) are found to be sensitive to the maximum stress intensity factor and load ratio. Similar to other ceramic materials, the long crack fatigue threshold, ΔK_{TH}, is found to be of the order of 45% of K_{Ic}, and enhanced with increasing fracture toughness. A unique growth law strongly dependent on the K_{max} and modestly on ΔK is established. Possible mechanisms for cyclic crack growth in whisker-reinforced zirconia composite materials are discussed. © 1997 Elsevier Science Limited.

1 Introduction

Recent studies have provided convincing evidence of the susceptibility of a wide range of ceramics and ceramic matrix composites (CMCs) to mechanical degradation under cyclic loading conditions. The majority of studies reported to date were on bending fatigue using smooth specimens,[1-15] and on fatigue crack growth using compact tension specimens.[16-22] Data now existing indicate reduced lifetimes during cyclic fatigue stress/life (S/N) testing and significant cyclic fatigue crack growth at loads less than those required for environmentally enhanced (static fatigue) crack growth during fracture mechanics studies in monolithic and composite systems, including Mg-PSZ, Al_2O_3, TZP, Si_3N_4, LAS/SiC$_F$, Si_3N_4/SiC$_F$. For example, cyclic fatigue crack propagation rates of long cracks in ceramics have been shown to be power-law dependent on the applied stress intensity.

In the simplest form, the growth increment per cyclic (da/dN) has been related to the applied stress-intensity range (ΔK) via a Paris power-law expression.[23]

$$\frac{da}{dN} = C(\Delta K)^m \qquad (1)$$

where C and m are experimentally measured scaling constants; however, the value of m can be far higher (i.e. in the range ~15 to 50) than the exponents of ~2 to 4 typically observed in metals. While the precise micromechanisms for such cyclic fatigue are still unclear, such characteristics of fatigue degradation appear, however, to be qualitatively the general case. A number of mechanisms have been postulated to explain fatigue crack growth in ceramics (e.g. Ref. 24). At the present time, considerable confusion on the interpretation of the fatigue crack growth rate data still exists and because of limited mechanistic data, precise mechanisms remain elusive. For example, the critical role of the unloading cycle in degrading the bridging zone or damaging materials ahead of the crack-tip remains unclear.

In the present study, first examination of the cyclic fatigue crack growth of SiC-whisker-reinforced 3Y-TZP(SiC$_w$/3Y-TZP) composites is reported. New experimental results on a whisker-reinforced transforming ceramic would add to the body of knowledge on the cyclic fatigue behaviour of toughened ceramics. Our experiments were performed using four-point bending specimens, cyclically stressed under the constant peak load condition. Two kinds of R ratios, defined as the ratio of the minimum stress intensity factor to the maximum stress intensity factor, were studied in order to provide insight into the relative importance of mean stress and stress amplitude. Detailed fractography of the resulting fatigue fracture surfaces is compared with those of

monotonically loaded cracks in order to provide some elucidation of the mechanisms of cyclic fatigue. Implications of the observed crack growth behaviour on possible mechanisms of cyclic fatigue in composites are discussed.

2 Experimental Procedure

2.1 Materials

Cyclic crack growth experiments were conducted on SiC-whisker-reinforced 3Y-TZP composites with 10, 20 and 30 vol% SiC whiskers, fabricated by dispersion processing and hot-pressing at 1550°C for 40 min. The resulting microstructures consisted of 0·65 μm diameter 3Y-TZP grains, and a density of 99% of the theoretical, with a uniform dispersion of 0·2~0·8 μm diameter SiC whiskers, with aspect ratios of up to 100, and predominantly of β form. Whiskers tend to be oriented perpendicular to the hot pressing direction. The fabrication process has been shown to minimize flaw populations and promote uniform microstructures. Some basic information and mechanical properties are listed in Table 1.

2.2 Test methods

2.2.1 Cyclic fatigue

Single-edge-notched bend specimens were used for the crack growth experiments, with the hot-pressing direction being parallel to the crack front. The specimens were of the following dimensions: length, S=40 mm; width, W=8·0 mm; thickness, B=5 mm; initial notch length to specimen width ratio, a_0/W =0·25; and notch root radius, ρ=75 μm. Before testing, both side surfaces of the specimens were polished up to 6-μm finish, using diamond wheels. After polishing, specimens were subjected to uniaxial cyclic compression in a Shimadzu Servopulser fatigue machine to introduce a stable mode I fatigue crack at the root of the notch. The cyclic compression loading frequency was 10 Hz (triangular wave form), and the maximum and minimum values of the nominal far-field compressive stress imposed on the specimen were σ_{max}= −40 MPa and σ_{min}= −400 MPa, respectively. The fatigue cracks propagated in a stable manner over

distances of approximately 300 μm, 456 μm, and 490 μm ahead of the notch tip in the 10, 20 and 30 vol% SiCw/3Y-TZP composites, respectively, before arresting completely after nearly 200,000 compression cycles.

Following precracking in cyclic compression, these specimens were heated to 1000°C for 30 min in order to relieve the residual stress, and then the edge-cracked specimens were subjected to fatigue crack growth in cyclic tension in a four-point-bend loading configuration (with the notch and the fatigue precrack on the tensile side of the bend specimen). The bend fixture had an inner span of 10 mm and an outer span of 30 mm. For the fatigue tests, load was cycled between a maximum (P_{max}) and a minimum tension load (P_{min}). All the tests were performed at room temperature and 40% relative humidity at a cyclic frequency, f, of 10 Hz and a tensile load ratios, $R = P_{min}/P_{max}$, of 0·1 and 0·3, respectively.

Crack lengths were measured *in situ* using a direct current potential drop technique. Further details on crack monitoring can be found in Ref. 25. Using this technique, it is possible to monitor crack lengths continuously in ceramics to a resolution of better than ±3 μm.

For four-point bending specimen, stress intensity factors were evaluated by means of the following equation:[26]

$$K = \beta F P \sqrt{\pi a} \qquad (2)$$

where

$$\beta = \frac{3(L - 1)}{2BW^2} \qquad (3)$$

$$F = 1·122 - 1·40(a/W) + 7·33(a/W)^2$$
$$- 13·08(a/W)^3 + 14·0(a/W)^4 \qquad (4)$$

and P is the applied load, L is the length of the outer span, l is the length of the inner span, B is the thickness, W is the depth, and a is the crack length.

2.2.2 Fractography

The fracture surfaces were covered with a gold–palladium coating and were examined in a scanning electron microscope (SEM). In addition, thin

Table 1. Mechanical properties of SiCw/Y-TZP composites

Volume fraction of SiC whiskers (%)	K_{Ic}[a] $(MPa\,m^{1/2})$	Bending strength (MPa)	Young's modulus (GPa)
10	8·50	850	220
20	6·42	795	230
30	6·89	757	240

[a]K_{Ic} is determined by single-edge-notched specimen.

sections were sliced out of the fatigue samples at the crack-tip region for transmission electron microscopy (TEM) analysis; 3-mm-diameter discs 100 μm thick, were cut from these slices using an ultrasonic core drill such that the crack-tip was located at the centre of the discs were polished, dimpled to approximately 30 μm, and then ion-milled. In order to ensure that the damage observed in the crack tip region was caused by the fatigue loading and not by the TEM specimen preparation techniques, TEM foils were also prepared from the as-received untested material, using the same foil preparation techniques, and examined for comparison purposes. The X-ray diffraction was also used to analyse the fraction of tetragonal to monoclinic transformation in the fractured samples under static and cyclic loading.

3 Results and Discussion

3.1 Constant amplitude crack growth behaviour

3.1.1 Growth rate behaviour

Cyclic fatigue growth data are plotted in Fig. 1 as a function of the stress intensity range (ΔK), for 10, 20 and 30 vol% SiCw/3Y-TZP composites, respectively. It is evident that the cyclic fatigue crack growth of the whisker-reinforced transforming ceramic composites also displays a power-law dependence on the stress intensity range. Similar to metallic materials and in agreement with data
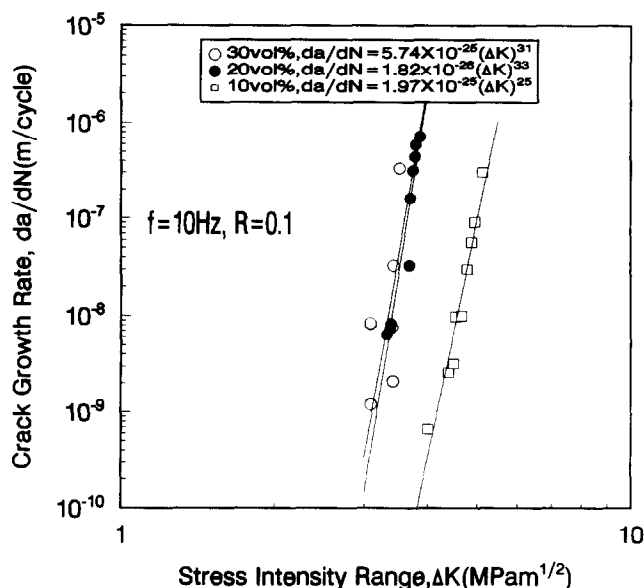

Fig. 1. Cyclic fatigue crack growth rates, da/dN, as a function of the applied stress intensity range ΔK for SiCw/Y-TZP composites. Data obtained for long cracks on four-point bending specimens in a room air environment at 10 Hz with a constant load ratio ($R = K_{min}/K_{max}$) of 0·1. For 10 vol% SiCw/Y-TZP:K_{max}=5·71 MPa m$^{1/2}$; for 20 vol%SiCw/Y-TZP: K_{max}=4·30 MPa m$^{1/2}$; for 30 vol%SiCw/Y-TZP:K_{max}=3·83 MPa m$^{1/2}$.

from a range of other ceramics, crack growth rates can be fitted to a conventional Paris law relationship of the form shown in eqn (1). However, the exponent m is considerably larger than reported for metals, i.e. in the range 25 to 33 (as opposed to 2 to 4 for metals[27]). The value of the fatigue threshold, measured at a maximum growth rate of 10^{-10} m cycle^{-1}, was found to be approximately 45% of K_{Ic}. Values of C, m and ΔK_{TH} for each SiCw/Y-TZP composite fabricated in this study are listed in Table 2. It can be seen that the material with 10 vol% SiC whiskers has a higher toughness and a lower crack growth rate for the same ΔK as the two other materials These results show that resistance to cyclic fatigue crack growth in composites is enhanced with increasing fracture toughness. From Table 1, the results indicate that the addition of whiskers to Y-TZP at around 10 vol% leads to an increase in both the fracture strength and toughness of the Y-TZP. The highest bend strength and toughness are thought to be mainly related to its large grain size and also to the homogeneous distribution of whiskers in the matrix.[25] The larger grain size favours a higher phase transformation volume, while the homogeneous distribution of the whiskers limits the whisker agglomeration effect. Above 20 vol% whisker content, the fracture strength and toughness decrease. One of the main reasons for this reduction is the high tensile stresses in the matrix due to the thermal mismatch. Whiskers clustering may be another reason for the reduction. Whisker agglomerates are usually large in size and will probably act as the origin of fracture.

To ascertain the contributions from cyclic versus static fatigue, we compared crack growth under a constant load and under a cyclic load as shown in Fig. 2. Crack growth was allowed to proceed under a cyclic loading until point B in Fig. 2. Between B and C, under sustained loading, there was no crack growth even though the stress intensity held constant at the same value of K_{max}(=3·9 MPa m$^{1/2}$). Crack growth later restarted at point C when the cyclic load was resumed at the same maximum stress intensity factor. As in other studies (e.g. Refs 16, 18), crack growth was shown to be a true cyclic fatigue phenomenon, with crack advance dependent on both the loading and unloading cycle, rather than environmentally enhanced (static fatigue) cracking at maximum load. In general, the experimental conditions of the present study were chosen so that static fatigue could be ignored compared to the cyclic fatigue effect.

3.1.2 The roles of K_{max} and ΔK

Figure 3(a) shows the fatigue crack growth rate data (da/dN) as a function of stress intensity range

Table 2. Values of C and m (in eqn (1)) and the threshold ΔK_{TH} for SiCw/Y-TZP composites

Whisker content (vol%)	K_{IC} ($MPa\ m^{1/2}$)	C ((m cycle^{-1} ($MPa\ m^{1/2}$)$^{-m}$)	m	$\Delta K_{TH}{}^a$ ($MPa\ m^{1/2}$)
10	8·50	$1·97 \times 10^{-25}$	25	3·82
20	6·42	$1·82 \times 10^{-26}$	33	2·86
30	6·89	$5·74 \times 10^{-25}$	31	3·09

$^a \Delta K_{TH}$ is determined at $da/dN = 10^{-10}$ m cycle^{-1}.

(ΔK) in the 30 vol% SiCw/Y-TZP composite, for two load ratios(R). It is evident that higher crack growth rate occurs when the R ratio is increased. When the crack growth rate is replotted as a function of the maximum stress intensity factor (K_{max}), the differences are significantly minimized, and the data appear to fit a single curve (Fig. 3(b)). These results agree with the findings of S. Y. Liu,[28,29] that a strong effect of the R ratio on fatigue life was observed and attributed to the strong dependence on the maximum stress. Taking a similar approach, we find that this strong dependence can be largely attributed to a strong dependence on the maximum stress intensity factor (K_{max}), in addition to ΔK. Thus, the fatigue growth rate can be represented by the following equation:[30]

$$da/dN = A'(K_{max})^n (\Delta K)^p \qquad (5)$$

where A' is a scaling constant which is independent of K_{max}, ΔK and R, and n and p are experimentally determined crack growth exponents. To interpret experiments at constant load ratio, it is more convenient to rewrite eqn (5) using $K_{max} = \Delta K/(1-R)$, to give the usual form of the Paris equation:[23]

$$da/dN = A'/(1-R)^n (\Delta K)^{(n+p)} \qquad (6)$$

where for constant R, the values of C and m from eqn (1) are
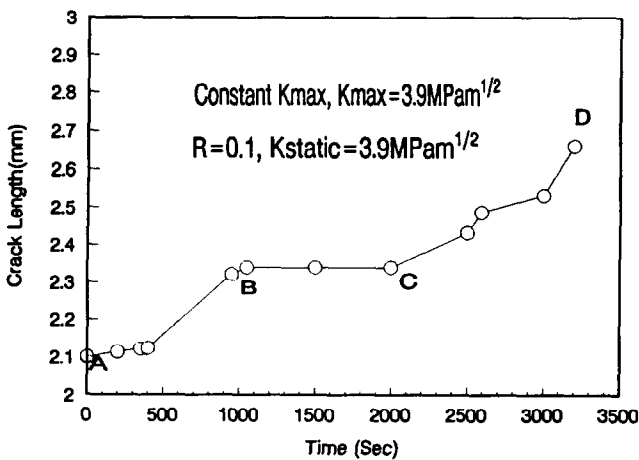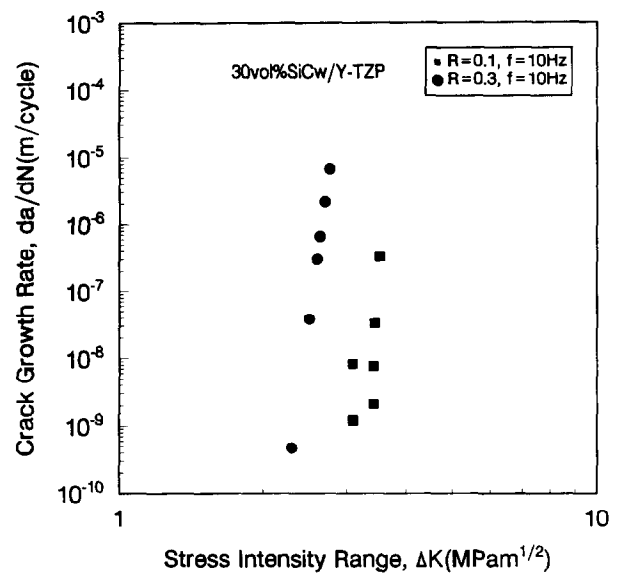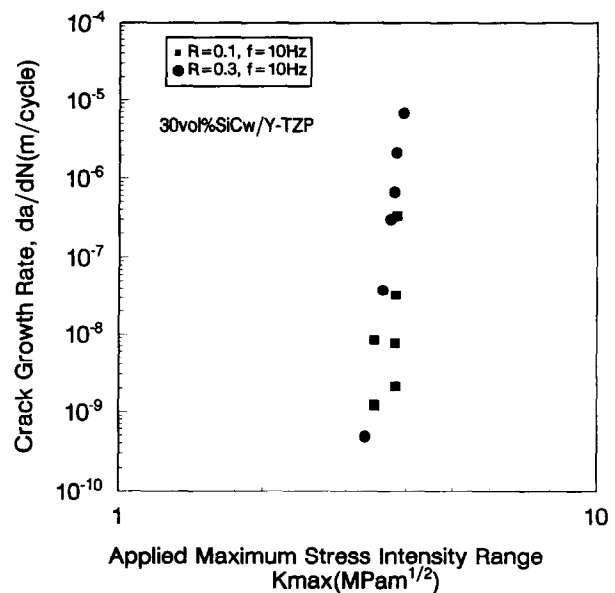
$$C = A'/[(1-R)]^n \qquad (7a)$$

$$m = n+p \qquad (7b)$$

A regression fit of eqn (5) to the data in Fig. 3 (b) yields values of $n = 29$ and $p = 2$ for this material. It is apparent that, unlike metals, cyclic fatigue

(a)

(b)

Fig. 3. (a) Fatigue crack growth rates versus ΔK of 30 vol% SiCw/Y-TZP, (b) fatigue crack growth rates versus K_{max} of 30 vol% SiCw/Y-TZP. (For $R=0·1$, $K_{max}=3·83$ MPa m$^{1/2}$ and for $R=0·3$, $K_{max}=3·95$ MPa m$^{1/2}$.)

Fig. 2. Crack length during sustained and cyclic loading.

crack growth rates in ceramics show a far greater dependence on K_{max} than on ΔK.

3.1.3 Fractographic observations

The transgranular nature of fatigue fracture surfaces was clearly evident from scanning electron microscopy (SEM) (Fig. 4), nominally similar to that obtained under a monotonic loading condition. Regions of abrasion and a large number of 'pullout' SiC whiskers were also apparent on the cyclic fracture surfaces (Fig. 4(a)), suggesting that the effect of cyclic loading may lead to a progressive weakening of the whisker/matrix interfaces, resulting in the larger pullout lengths observed. At higher magnification, regions of cyclic crack growth, which are a mixture of predominantly intergranular of smaller grains and transgranular of larger grains (Fig. 4(b)), are clearly the same as the transgranular monotonic fracture region. These observations are consistent with some previous investigation on a different system.[30] Unlike many metals and polymers, no evidence of fatigue striations or crack arrest markings is apparent on the fatigue fracture surfaces.

X-ray diffraction of the fracture surfaces on 10 vol% and 20 vol% SiCw/Y-TZP composites showed that little monoclinic phase was detected in the static fatigue specimen, although 16 and 20% of transformation from tetragonal to monoclinic was observed for the overall cyclic fatigue specimens, respectively. Partially stabilized tetragonal phase is known to transform to monoclinic phase by stressing. These results showed that the cyclic stress gives rise to much more enhanced phase transformation at the crack tip than the static stress does in these composites.

Figure 5 shows a bright-field transmission electron micrograph of microcracks at the grain-boundary termination of the monoclinic twin laths in a partially transformed tetragonal grain in the transformation zone of an SiCw/Y-TZP fatigue specimen.

3.2 Mechanisms of fatigue crack growth

In metals, mechanisms of cyclic fatigue have been based primarily on crack tip dislocation activity leading to crack advance via such processes as alternating blunting and resharpening of the crack tip.[24] Accordingly, the denial of the existence of a true fatigue effect in ceramics has been based in the past on the very limited crack tip plasticity in these materials. However, it is now apparent that other inelastic deformation mechanisms may prevail; these mechanisms include microcracking and transformation 'plasticity' in monolithic materials, the frictional sliding or controlled debonding between the reinforcement phase and ceramic matrix in brittle fibre or whisker-reinforcement composites. Because of the paucity of mechanistic data, precise mechanisms remain elusive. In ceramic matrix composites reinforced with whiskers, careful control of the reinforcement matrix interface

Fig. 4. SEM micrograph of a fracture surface for 30 vol% SiCw/Y-TZP. (a) From left to right, the regions of fast fracture, four-point bending, compression-compression, and notch respectively; (b) a higher magnification region of four-point bending fatigue.
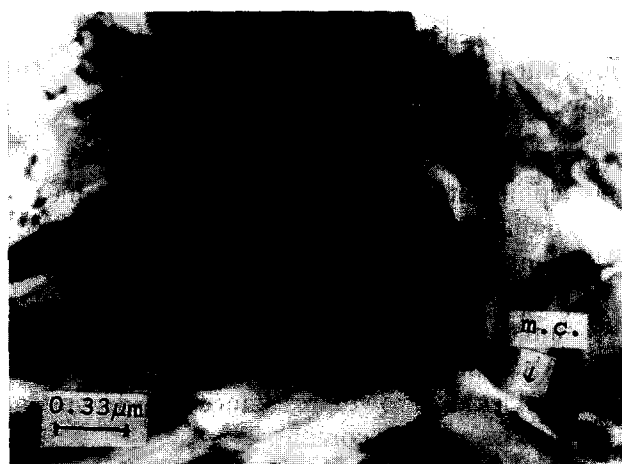

Fig. 5. Bright-field transmission electron micrograph showing microcracks at the grain-boundary termination of the monoclinic twin laths in a partially transformed tetragonal grain in the transformation zone of SiCw/Y-TZP fatigue specimen.

strength during processing is required to provide debonding and controlled pullout of the reinforcement whiskers in the wake of a crack. The resulting bridging zone exerts closing traction on the crack surfaces and hence shields the crack tip from the applied stress. These materials may be expected to be susceptible to cyclic fatigue effects.[30]

In the present study, the close similarity of fracture surfaces resulting from cyclic and monotonic loading suggests that fracture modes similar to those under monotonic loading (static modes) may be operating. In this case, crack-growth rates during cyclic loading may be expected to display a marked sensitivity to the maximum stress intensity factor, K_{max}, or the load ratio, R, in addition to ΔK, as shown in eqn (5). It is also very similar to fatigue in metals at high growth rates where K_{max} approaches the fracture toughness, K_{Ic}. In the present materials, 'static' crack-advance mechanisms appear to be dominant over the entire range of cyclic crack growth rates, with the smaller dependence on ΔK arising from the crack-tip shielding.

In present study, experimental results have identified microcracking as the most likely mechanism for plastic strain accumulation and it may be responsible for fatigue damage and crack growth. This microcracking mechanism can be regarded as pseudoplastic, because it is distinct from the classical plastic deformation due to dislocation slip. In terms of the magnitude of strain, it is also much smaller than the classical plastic deformation in metals. Nevertheless, from a mechanical point of view, this inelastic deformation can still be responsible for crack tip deformation and damage.[28]

4 Conclusions

Based on a study of the growth of fatigue cracks in SiC-whisker-reinforced Y-TZP ceramic matrix composites under four-point bending loading, the following conclusions can be drawn:

(1) Fatigue crack growth in SiCw/Y-TZP composites is shown to be a mechanically induced cyclic process. Growth rate (da/dN) can be described in terms of a power-law function of the stress intensity range, with an exponent m in the range of 25 to 33. Also, the results show that both toughness and crack growth resistance are dependent on the whisker content.

(2) A threshold for cyclic fatigue crack growth, ΔK_{TH}, was found to be approximately 45% of K_{Ic}, similar to the behaviour of other ceramics.

(3) Fatigue crack growth in composites is suggested to follow a microplastic-related mechanism. Microcracking may be a plausible general explanation for microplasticity.

References

1. Krohn, D. A. & Hasselman, D. P. H., Static and cyclic fatigue behavior of a polycrystalline alumina. *J. Am. Ceram. Soc.*, **55** (1972) 208–211.
2. Kosswsky, R., Cyclic fatigue of hot-pressed Si₃N₄. *J. Am. Ceram. Soc.*, **56** (1973) 531–555.
3. Chen, C. P. & Knapp, W. J., Fatigue fracture of an alumina ceramic at several temperatures. In *Fracture Mechanics of Ceramics*, Vol. 2, ed. R. C. Bradt, A. G. Evans, D. P. Hasselman & F. F. Lange. Plenum Press, New York, 1973, pp. 691–707.
4. Ko, H. N., Fatigue strength of sintered Al₂O₃ under rotary bending. *J. Mater. Sci. Lett.*, **63** (1986) 464–466.
5. Ko, H. N., Cyclic fatigue behavior of sintered Al₂O₃ under rotary bending. *J. Mater. Sci. Lett.*, **64** (1987) 801–805.
6. Maekawa, I., Shibata, H. & Kobayashi, A., Bending fatigue of Al₂O₃-ZrO₂ ceramics. *J. Soc. Mater. Sci. Jpn*, **36** (1987) 1116–1127.
7. Zelizko, V. & Swain, M. V., Influences of surface preparation on the rotating flexural fatigue of Mg-PSZ. *J. Mater. Sci.*, **23** (1988) 1077–1082.
8. Swain, M. V. & Zelizko, V., Comparison of static and cyclic fatigue on Mg-PSZ alloys. In *Advances in Ceramics*. Vol. 24B, *Science and Technology of Zirconia III*, ed. S. Somiya, N. Yamamoto & H. Nanagida. American Ceramic Society, Westeville, OH, 1988, pp. 595–606.
9. Takatsu, M., Kamiya, H., Ohya, K., Ogura, K. & Kinoshita, T., Effect of vibrating cyclic fatigue properties of ceramics from stress load condition. *J. Jpn Ceram. Soc.*, **96** (1988) 990–996.
10. Masuda, M., Yamada, N., Soma, T., Matsui, M. & Oda, I., Fatigue of ceramics, Part 2—Cyclic fatigue properties of sintered Si₃N₄ at room temperature. *J. Jpn Ceram. Soc.*, **97** (1989) 520–524.
11. Sylva, L. A. & Suresh, S., Crack growth in transforming-ceramics under cyclic tensile load. *J. Mater. Sci.*, **24** (1989) 1729–1738.
12. Takatsu, M., Ohya, K. & Ando, M., The relationship between cyclic fatigue properties and microstructure of silicon nitride ceramics. *J. Jpn Ceram. Soc.*, **98** (1990) 490–498.
13. Kamiya, H., Ohya, M., Ando, M. & Hattori, A., Effect of microstructure on cyclic fatigue properties of Al₂O₃ ceramics and Al₂O₃ composites. *J. Jpn Ceram. Soc.*, **98** (1990) 456–463.
14. Steffen, A. A., Dauskardt, R. H. & Ritchie, R. O., Cyclic fatigue crack propagation in ceramics: Long and small crack behavior. *Fatigue 90, Proc. Fourth International Conference on Fatigue and Fatigue Thresholds*, ed. H. Kitagawa & T. Tanaka. Materials and Component Engineering Publications Ltd, Birmingham, UK, 1990, pp. 745–752.
15. Cardona, D. C. & Beevers, C. J., Fatigue behavior of zirconia–ceria alloys. *Fatigue 90, Proc. Fourth International Conference on Fatigue and Fatigue Thresholds*, ed. H. Kitagawa & T. Tanaka. Materials and Component Engineering Publications Ltd, Birmingham, UK, 1990, pp. 1023–1029.
16. Dauskardt, R. H., Marshall, D. B. & Ritchie, R. O., Cyclic fatigue-crack propagation in magnesia-partially-stabilized zirconia ceramics. *J. Am. Ceram. Soc.*, **73** (1990) 893–903.
17. Dauskardt, R. H., Yu, W. & Ritchie, R. O., Fatigue crack propagation in transformation-toughened zirconia-ceramic. *J. Am. Ceram. Soc.*, **70** (1987) C-248–C-252.

18. Reece, M. J., Guiu, F. & Sammur, M. F. R., Cyclic fatigue crack propagation in alumina under direct tension–compression loading. *J. Am. Ceram. Soc.*, **72** (1989) 348–352.

19. Kishimoto, H., Ueno, A. & Kawamoto, H., Crack propagation behavior of Si_3N_4 under cyclic load—influence of difference in materials. *Fatigue 90. Proc. Fourth International Conference on Fatigue and Fatigue Thresholds*, ed. H. Kitagawa & T. Tanaka. Materials and Component Engineering Publications Ltd, Birmingham, UK, 1990, pp. 727–732.

20. Ueno, A., Kishimoto, H., Kawamoto, H. & Asakura, M., Crack propagation behavior of sintered silicon nitride under cyclic load of high stress ratio and high frequency. *Fatigue 90, Proc. Fourth International Conference on Fatigue and Fatigue Thresholds*, ed. H. Kitagawa & T. Tanaka. Materials and Component Engineering Publications Ltd, Birmingham, UK, 1990, pp. 733–738.

21. Dauskardt, R. H., Carter, W. C., Veirs, D. K. & Ritchie, R. O., Transient subcritical crack growth behavior in transformation-toughened ceramics. *Acta Metall.*, in press.

22. Tsai, J. F., Yu, C. S. & Shetty, D. K., Fatigue crack propagation in ceria-partially-stabilized zirconia (Ce-TZP)– alumina composites. *J. Am. Ceram. Soc.*, **73** (1990) 2992–3001.

23. Paris, P. C. & Erdogan, F., A critical analysis of crack propagation law. *J. Basic. Engng, Trans. ASME*, **85** (1963) 528–534.

24. Ritchie, R. O. & Dauskardt, R. H., Cyclic fatigue of ceramics: A fracture mechanics approach to subcritical crack growth and life prediction. *J. Ceram. Soc. Jpn*, **99** (1991) 1047–1062.

25. Guo-Dong Zhan, Toughness and fatigue behavior of particle and whisker-reinforced 3Y-TZP ceramic composites. PhD Dissertation, Huazhong University of Science and Technology, 1993.

26. Okazaki, M., McEvily, A. J. & Tanaka, T., On the mechanism of fatigue crack growth in silicon nitride. *Metall. Trans.*, **22A** (1991) 1425–1434.

27. Dauskardt, R. H., Haubensak, F. & Ritchie, R. O., On the interpretation of the fractual character of fracture surfaces. *Acta Metall. Mater.*, **38** (1990) 143–159.

28. Liu, S. Y. & Chen, I.-W., Fatigue of yttria-stabilized zirconia: II. Crack propagation, fatigue striations, and short-crack behavior. *J. Am. Ceram. Soc.*, **74** (1991) 1206–1216.

29. Liu, S. Y. & Chen, I. W., Fatigue of yttria-stabilized zirconia: I. Fatigue damage, fracture origins, and lifetime prediction. *J. Am. Ceram. Soc.*, **74** (1991) 1197–1205.

30. Dauskardt, R. H., James, M. R., Porter, J. R. & Ritchie, R. O., Cyclic fatigue-crack growth in a SiC-whisker-reinforced alumina ceramic composite: Long and small crack behavior. *J. Am. Ceram. Soc.*, **75** (1992) 759–771.